neuroReport

NeuroReport 9, 893–897 (1998)

Neural networks for generation and suppression of alpha rhythm: a PET study

Norihiro Sadato,[CA] Satoshi Nakamura, Tsutomu Oohashi,[1] Emi Nishina,[2] Yoshitaka Fuwamoto,[3] Atsuo Waki and Yoshiharu Yonekura

Biomedical Imaging Research Center, Fukui Medical University, 23 Shimoaizuki, Matsuoka, Yoshida, Fukui 910-11; [1]ATR Human Information Processing Research Laboratories, Kyoto; [2]National Institute of Multimedia Education, Chiba; [3]Foundation for Advancement of International Science, Tsukuba, Japan

[CA]Corresponding Author

To study neuronal activities that influence the generation of the alpha rhythm, we used positron emission tomography and simultaneous recording of the electroencephalogram (EEG) in normal volunteers and under passive conditions. A negative correlation between regional cerebral blood flow and alpha power was found in the occipital cortex, consistent with the visual modality-specific reactivity of the alpha rhythm. A positive correlation was found in the pons, midbrain, hypothalamus, amygdala, the basal prefrontal cortex, insula and the right dorsal premotor cortex. Neuronal activities of the brain stem and limbic system that are positively correlated with alpha power may provide an anatomical basis for studies of the relationship between emotional state and brain rhythm in health and disease.
***NeuroReport* 9: 893–897 © 1998 Rapid Science Ltd.**

Key words: Alpha rhythm; Cerebral blood flow; Electroencephalogram; Positron emission tomography

Introduction

The alpha rhythm on the electroencephalogram (EEG) is a macroscopic oscillation of the potentials generated by electric currents developing in the brain with a frequency of 8–13 Hz which occurs in relaxed but alert subjects. These potentials have been explored as a possible indicator of emotional as well as arousal states.[1] Although the role of the visual projection cortex and thalamus in the generation of the alpha rhythm has been emphasized,[2] its physiological meaning or the involvement of other brain regions is still unclear. The purpose of this study was to depict functional neuroanatomy that influence the generation of the alpha rhythm by simultaneous measurements of EEG and cerebral blood flow (rCBF).

Materials and Methods

Subjects were eight normal volunteers (three women and five men), aged 24–37 (mean 29.9) years. All subjects were right-handed according to the Edinburgh inventory.[3] The protocol was approved by the Ethical Committee of Fukui Medical University, and all subjects gave their written informed consent for the study.

A small plastic catheter was placed in the cubital vein of each subject's left arm for injection of the radioisotope. During PET scanning, the subjects lay in a supine position with their eyes open and their heads immobilized with an elastic band and sponge cushions. Subjects were equipped with earphones, and electrodes were applied to 12 scalp sites according to the international 10-20 system of electrode placement, with linked earlobe electrodes used as a reference, and a filter setting of 1–60 Hz (–3 dB). The EEGs were recorded in digital format and data were acquired using the WEE-6112 telemetric system (Nihon Koden, Tokyo, Japan).

The experiment consisted of three PET studies performed on the same subjects at 6-month intervals. The eight volunteers each underwent 10 consecutive PET scans with a 10 min interval between scans. A complete session consisted of two rest scans and eight scans with a music condition. For the rest scans, subjects lay quietly, watching a static picture on a board in front of them. The subjects were instructed

not to move nor close their eyes during each scan. Spontaneous eye blink was allowed. No attempt was made to control the subjects' thought content or attention during rest. For the music condition, subjects listened to traditional Gamelan music containing a non-audible, high-frequency (> 22 kHz) component. For the purpose of other research projects, the music was presented as a full range of sound or high cut sound through earphones or speakers. The music began ~50–90 s before the start of the scan and continued for 200 s. No response of the subjects was requested during the session. The EEG was continuously recorded throughout the approximately 90 min of each PET study.

PET scanning was performed with a General Electric Advance tomograph (GE/Yokogawa Medical System, Tokyo, Japan) with the interslice septa retracted. The scanner acquires 35 slices with interslice spacing of 4.25 mm. A 10 min transmission scan using two rotating Ge-68 sources was performed for attenuation correction. Images of cerebral blood flow were obtained by summing the activity occurring within the 90 s period following the initial increase in cerebral radioactivity after an i.v. bolus injection of 10 mCi ^{15}O-labeled water. The images were reconstructed with Hanning filters, giving transaxial and axial resolutions of 6 and 10 mm (full-width at half-maximum, FWHM), respectively. The field of view and pixel size of the reconstructed images were 256 mm and 2 mm, respectively. No arterial blood sampling was performed, and thus the images collected were those of tissue activity. Tissue activity recorded by this method is nearly linearly related to rCBF.[4] Lack of contamination of tissue activity images of the brain by the radioactivity of the extracranial structures such as extraocular muscles was ensured by visual inspection.

EEGs data of 120 s in duration from ~30 s before the start of each PET scan were used for correlation analysis between rCBF and the EEG. The alpha-potential at each electrode position was obtained by integrating spectral densities in the EEG band of 8–13 Hz in the Fourier domain. To eliminate artifacts caused by eye movement, only the data from the posterior one-third of the scalp were selected and averaged. The spatially averaged alpha-potential for each condition in each subject was normalized with respect to the mean value across all conditions in all three studies in each subject to eliminate intersubject differences.

The PET and EEG data were analyzed with statistical parametric mapping (SPM: from the Wellcome Dept. of Cognitive Neurology, London, UK) implemented in Matlab (Mathworks Inc., Sherborn MA, USA)[5]. The PET scans from each subject's three studies were realigned, with the first image used as a reference. Following realignment, all images were transformed into a standard stereotaxic space.[6] Each image was smoothed to account for the variation in normal gyral anatomy, using a Gaussian filter (FWHMx × FWHMy × FWHMz = 20 × 20 × 20 mm). After the appropriate design matrix was specified, the condition, subject and effect of the covariate, that is, the amplitude of the alpha-wave, were estimated according to the general linear model at each and every voxel, assuming a linear relationship between rCBF and the covariate. The effect of global CBF was eliminated by proportional scaling. The resulting set of voxel values for each contrast constitutes a statistical parametric map of the t statistic SPM{t}. The SPM{t} was transformed to the unit normal distribution (SPM{Z}). The threshold of SPM{Z} was set at $Z > 3.09$. The resulting foci were characterized in terms of spatial extent (k) and peak height (u). The significance of each region was estimated using a distributional approximation from the theory of Gaussian fields.[5] This characterization is expressed in terms of the probability that a region of the observed number of voxels could have occurred by chance [P(nmax > k)] giving the corrected *p*-values at cluster levels for multiple comparisons over the entire volume analyzed, or that the observed peak height could have occurred by chance [P(Zmax > u)] giving the corrected *p*-values at voxel levels. A corrected *p*-value of < 0.05 was used as a statistical threshold.[5]

Results

A strong positive correlation between rCBF and the alpha power spectrum was found in the brain stem extending from the upper pons to the midbrain on the left. The limbic system, including the hypothalamus, right amygdala, and right thalamus, extending to the basal prefrontal cortex and insula mainly on the right, also showed a positive correlation. On the cerebral convexity, the right dorsal premotor cortex extending to the right supplementary motor area showed a positive correlation (Fig. 1A, Table 1). A negative correlation between rCBF and alpha power was found in the bilateral occipital cortex, including the primary and association visual cortex. The dorsomedial prefrontal cortex on the left also showed a negative correlation (Fig. 1B, Table 1). Extensive involvement of the primary and association visual cortex is consistent with the finding that the alpha rhythm can be suppressed not only by opening of the eyes but also by visual imagery, which suggests that higher visual processing is necessary for suppression of the alpha rhythm.[7]

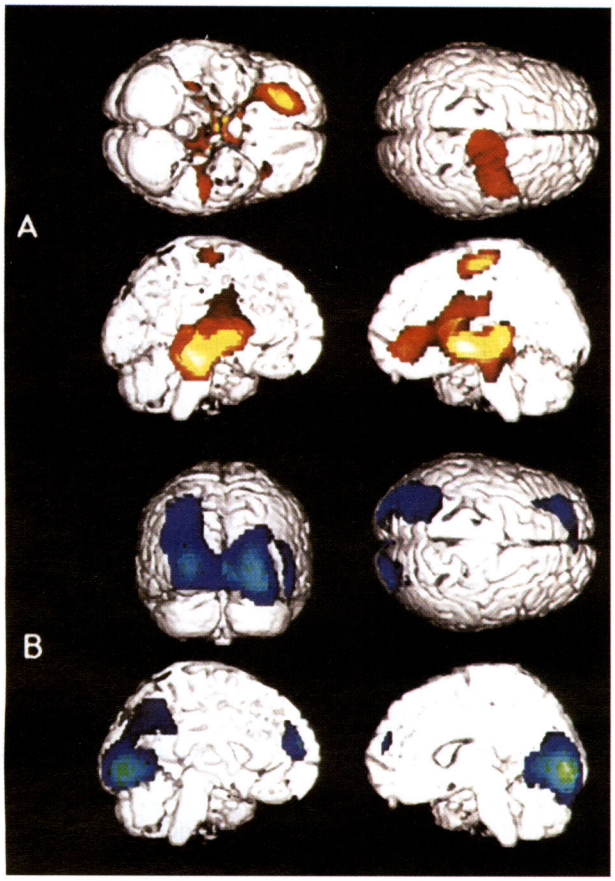

FIG. 1. Statistical parametric maps of positive (**A**, yellow) and negative (**B**, blue) correlation between rCBF and EEG power of the alpha frequency range (8–13 Hz), superimposed on surface-rendered high-resolution MRI. Areas of $Z > 3.09$ with cluster-level significance of $p < 0.05$ with corrections for multiple comparisons are shown.

Discussion

Regional cerebral blood flow has been used as an indirect measure of functional activity.[8] Measurement of rCBF using O^{15} water and PET has been well established based on the single-tissue compartment model for diffusible tracers. The required assumptions are that (1) water is freely diffusible, (2) the contribution to the signal in a region arising from arterial activity is negligible, (3) venous and tissue concentrations are negligibly different, and (4) both flow and distribution volume of the water are constant during the measurement period.[9] These assumptions are acceptable in at least physiologically normal brain tissue.[9] Hence the correlation observed in the present study is reflecting the change in the neuronal activities covaried with alpha power.

Although complete control of the eye movements was difficult, they are unlikely to affect the present results. First, contamination of EEG by eye movements was minimized by careful instruction to the subjects not to move their eyes during the session, and by using EEG data from posterior leads for the power analysis. Lambda waves, which occur in the occipital region during visual exploration, are independent of alpha rhythm[10] and unlikely to affect the alpha power. Second, contamination of tissue activity images by radiotracers accumulated in the extraocular muscles was denied by visual inspection of the original images. Finally, neuronal activity of frontal eye field is parallel with the frequency of saccadic eye movement but not the basal frontal cortex.[11] Hence a positive correlation between the basal frontal cortex and the alpha rhythm is not a spurious correlation with eye movements.

Although intraindividual variability of the power spectrum of the alpha rhythm may arise as the result of changes in experimental conditions (e.g. vigilance), or inherent random elements of the EEG, the test–retest reliability of spectral parameters of the alpha rhythm has been confirmed, and the normal alpha rhythm can be treated as an intraindividually stable trait.[12] In three separate tests over 2.5 years, healthy older adults showed no significant change in the percentage of power in the alpha rhythm.[13]

The mechanisms of generation of the alpha rhythm, based on an animal model, involve thalamocortioal and intracortical networks.[2] Alpha rhythms can be recorded from the visual cortex as well as the lateral geniculate and pulvinar nuclei.[14] Alpha rhythms from the visual cortex are generated by an equivalent dipole layer centered at layers IV and V in relatively small cortical areas that act as epicenters from which the potentials spread as much as 4 mm.[15] While coherence between alpha rhythms in the thalamus and cortex does exist, intracortical coherence at short distances is stronger.[14,15] Hence, there are both thalamocortical and cortico-cortical systems that interact in the generation of cortical alpha rhythms.[2] This is in contrast with natural sleep spindling (7–14 Hz), which shows an apparent similarity with the alpha rhythm. Natural sleep spindling appears in the early stages or sleep, in association with the blockade of synaptic transmission through the thalamus.[2] During the later stages of sleep, sleep spindling is progressively reduced and replaced by thalamocortical oscillations with slower frequencies, such as delta oscillation (1–4 Hz) and slow oscillation (< 1 Hz).[16] This transition is caused by progressive hyperpolarization of the thalamocortical cells due to disconnection from related cortical areas.[20] A recent PET study[17] showed that during slow-wave sleep the dorsal pons, mesencephalon, thalami, basal ganglia, orbital frontal cortex and anterior cingulate cortex were progressively deactivated as sleep stages progressed. The deactivation in the brain stem reflects the decrease in the firing rate of neurons of diffuse ascending brain stem systems, which leads to the hyperpolarization of thalamic nuclei, and the

Table 1. Correlation between regional cerebral blood flow and EEG power in the alpha frequency range (8–13 Hz)

Cluster level		Tailarach coordinates				Side	Location[a]
p	{k,Z}	x	y	z	Z[b]		
Positive correlation (height threshold Z > 3.09, extent threshold $p < 0.05$)							
< 0.001	{10941,7.70}	30	2	–4	7.70 (< 0.001)	rt	Insula
		–26	18	16	4.21 (0.015)	lt	Insula
		–12	–32	–12	6.75 (< 0.001)	lt	Midbrain
		48	0	44	6.19 (< 0.001)	rt	PMd (6)
		22	44	–8	6.13 (< 0.001)	rt	GFm (11)
		–26	–16	8	6.01 (< 0.001)	lt	Putamen
		30	–32	–4	5.68 (< 0.001)	rt	Gh
		16	–16	68	4.71 (0.002)	rt	SMA (6)
		–6	–30	–24	4.61 (0.003)	lt	Pons
		4	–4	–4	4.80 (0.001)	rt	Hypothalamus
		–4	–4	–4	4.16 (0.018)	lt	Hypothalamus
		–26	24	8	4.24 (0.013)	lt	GFi (45)
		12	–22	4	4.04 (0.027)	rt	Thalamus
		24	–4	–12	4.02 (0.028)	rt	Amygdala
Negative correlation (height threshold Z > 3.09, extent threshold $p < 0.05$)							
< 0.001	{7377,9.28}	26	–88	0	9.28 (< 0.001)	rt	GOi (18)
		–24	–86	4	7.17 (< 0.001)	lt	GOi (18)
		–30	–66	40	5.75 (< 0.001)	lt	GOs (18)
		10	–90	0	5.12 (< 0.001)	rt	Cu (17)
		–10	–90	0	4.71 (0.002)	lt	Cu (17)
		56	–60	–12	4.19 (0.016)	rt	GF (37)
< 0.001	{646,6.13}	–28	52	24	6.13 (< 0.001)	lt	GFs (10)
		–26	40	40	4.65 (0.003)	lt	GFs (8)

[a]Brodmann area according to Tailarach and Tourneaux.[6]
[b]Significance of activation at voxel level corrected for multiple comparisons.[6]
Cu, cuneus; GF, fusiform gyrus; GFi, inferior frontal gyrus; GFm, middle frontal gyrus; GFs, superior frontal gyrus; Gh, parahippocampal gyrus; GOi, inferior occipital gyrus; GOs, superior occipital gyrus; PMd, dorsal premotor cortex; SMA, supplementary motor area.

deactivation in the limbic and paralimbic cortices reflects cellular processes taking place during slow-wave sleep, that are modulated differently from other cortical mantles.[17]

The neuronal activity that was positively correlated with the alpha rhythm in the present study was observed in brain areas that were negatively correlated with sleep stages in the earlier study.[17] This might reflect the different mechanisms of generation of the alpha rhythms and activity on the sleep EEG. A positive correlation of neuronal activity in the midbrain and pons with alpha power is consistent with the blink-alpha neurocircuit hypothesized by Karson *et al.*,[18] who suggest that the eye blink rate is regulated through a common neural circuit that also regulates the alpha rhythm. The circuit begins in the rostral pons and involves subcortical structures (midbrain tectum, substantia nigra, lateral geniculate bodies) and the occipital cortex.[18] Linkage between the alpha rhythm and the eye blink rate has been clinically suggested. A study using magnetoencephalography[19] showed that the region of the posterior parietal cortex close to the midline, which produces the prominent magnetic alpha activity, was strongly activated in association with voluntary eye blinks. In schizophrenia, spontaneous blink rates are frequently elevated, and the alpha rhythm of the EEG is often absent or of low frequency. In two diseases involving abnormal dopaminergic activity, spontaneous blink rates are decreased in one (Parkinson's disease) and increased in the other (schizophrenia) and altered by the status of illness and treatment.[20] A study in non-human primates[21] showed that dopamine agonists acutely increased the blink rate, an effect that was dose-dependent[21] and blocked by sulpiride.[20] These findings suggest that the alpha rhythm may reflect central dopamine activity through the alpha-blink circuit in the brain stem.[18] As dopaminergic cell groups in the substantia nigra and ventral tegmental areas are subdivisions of arousal systems in which other neurotransmitter subgroups interact to control fluctuations in behavioral and autonomic activities during the awake state,[18] the alpha rhythm may reflect the arousal state through neural activities in the brain stem.

In the present study, alpha power was positively correlated with neuronal activity in the limbic system, including the hypothalamus and amygdala, extending to the basal prefrontal cortex. The anterior insula has extensive connections with limbic, paralimbic, olfactory, gustatory, and autonomic structures.[22] The anterior insula participates in the process of determining the affective tone of experience and behavior, which is consistent with its role in the modulation

of autonomic responses.[22] The orbitofrontal cortices are associated with social-affective and motivational aspects of frontal lobe function.[23] They are connected with the limbic system as well as the autonomic system.[24] Both the brain stem and the limbic forebrain mediate the stress response by their interactions with the neuroendocrine hypothalamic periventricular nucleus.[25] Hence, emotional states altered by stress responses or relaxation mediated by these neuronal networks may be reflected by the alpha rhythm through the blink-alpha neurocircuit, and thence the pacemakers in the thalamus.

Conclusion

Positive correlation between alpha power and neuronal activities in the brain stem and limbic system may provide a neuroanatomical basis for studies of the relationship between emotional state and alpha rhythm in health and disease.

References

1. Drennen WT and O'Reilly BK. *Percept Mot Skills* **62**, 467–474 (1986).
2. Steriade M, Gloor P, Llinas RR *et al. Electroencephalogr Clin Neurophysiol* **76**, 481–508 (1990).
3. Oldfield RC. *Neuropsychologia* **9**, 97–113 (1971).
4. Fox PT and Mintun MA. *J Nucl Med* **30**, 141–149 (1989).
5. Friston KJ, Holmes AP, Worsley KJ *et al. Hum Brain Mapp* **2**, 189–210 (1995).
6. Talairach J and Tournoux P. *Co-planar Stereotaxic Atlas of the Human Brain.* Translated by Rayport M. New York: Thieme, 1988.
7. Hari R and Salmelin R. *Trends Neurosci* **20**, 44–49 (1997).
8. Raichle ME. Circulatory and metabolic correlates of brain function in normal humans. In: Mountcastle VB, Plum F and Geiger SR, eds. *Handbook of Physiology. Section 1: The Nervous System. Volume V. Higher Functions of the Brain.* Bethesda: American Physiology Society, 1987: 643–674.
9. Lammertsma AA and Mazoyer BM. *Eur J Nucl Med* **16**, 807–812 (1990).
10. Niedermeyer E and Da Siva FL. *Electroencephalography: Basic Principles, Clinical Applications, and Related Fields.* Baltimore: Urban and Schwarzenberg, 1982: 84.
11. Paus T, Marrett S, Worsley KJ and Evans AC. *J Neurophysiol* **74**, 2179–2183 (1995).
12. Gasser T, Bacher P and Steinberg H. *Electroencephalogr Clin Neurophysiol* **60**, 312–319 (1985).
13. Coben LA, Danziger W and Storandt M. *Electroencephalogr Clin Neurophysiol* **61**, 101–112 (1985).
14. Da Silva FL, Van Lierop THMT, Schrijer CFM and Van Leeuwen WS. *Electroencephalogr Clin Neurophysiol* **35**, 627–639 (1973).
15. Da Silva FL and Van Leeuwen WS. *Neurosci Lett* **6**, 237–241 (1977).
16. Steriade M, McCormick DA and Sejnowski TJ. *Science* **262**, 679–685 (1993).
17. Maquet P, Degueldre C, Delfiore G *et al. J Neurosci* **17**, 2807–2812 (1997).
18. Karson CN, Dykman RA and Paige SR. *Schizophr Bull* **16**, 345–354. (1990).
19. Hari R, Salmelin R, Tissari SO *et al. Nature* **367**, 121–122 (1994).
20. Karson CN. *Brain* **106**, 643–653 (1983).
21. Kleven MS and Koek W. *J Pharmacol Exp The* **279**, 1211–1219 (1996).
22. Mesulam M-M and Mufson EJ. The insula of Reil in man and monkey: architectonics, connectivity, and function. In: Peters A and Jones EG, eds. *Cerebral Cortex.* New York: Plenum, 1985: 179–226.
23. Fuster JM. *The Prefrontal Cortex, Anatomy, Physiology, and Neuropsychology of the Frontal Lobe.* New York: Raven Press, 1989.
24. Goldman-Rakic PS. *Annu Rev Neurosci* **11**, 137–156 (1988).
25. Herman JP and Cullinan WE. *Trends Neurosci* **20**, 78–84 (1997).

Received 17 December 1997; accepted 11 January 1998

neuroReport

NeuroReport 8, 3775–3778 (1997)

A rapid brain metabolic change in infants detected by fMRI

Hiroki Yamada,[1,CA] Norihiro Sadato,[2] Yukuo Konishi,[3] Kouki Kimura,[3] Masato Tanaka,[1] Yoshiharu Yonekura[2] and Yasushi Ishii[1]

Department of [1]Radiology, [2]Biomedical Imaging Research Center, and [3]Department of Pediatrics, Fukui Medical School, Fukui, Japan

[CA]Corresponding Author

To determine developmental changes of activity-related metabolism in human visual cortex, we performed functional magnetic resonance imaging (fMRI) from the neonatal period. A rapid metabolic changing pattern accompanying normal human brain maturation was revealed by fMRI with photic stimulation. Infants older than 8 weeks of age showed a stimulus-related signal decrease in the visual cortex, whereas younger neonates showed a signal increase. This inversion of response in infants suggests a change in oxygen consumption during neuronal activation, which is related to rapid synapse formation and accompanying increased metabolism. fMRI can detect dynamic metabolic changes during the brain maturation, and provides a new clue in the detection of abnormal brain development or CNS plasticity.

Key words: Brain activation; Critical period; fMRI; Infant; Visual cortex

Introduction

The anatomy, function, and metabolism of the human brain changes rapidly in early life.[1–4] Since the principal brain substances for energy production are glucose and oxygen, indirect assessment of local energy requirements for maintenance processes and functional activity in resting condition in infants has been obtained by the measurement of regional cerebral metabolic rates for glucose (rCMRGlu) with positron emission tomography (PET).[4,5]

The development of functional magnetic resonance imaging (fMRI), which is a non-invasive imaging tool for detecting neuronal activity induced by the external stimuli, has enabled us to directly study human cerebral functional development. Blood oxygenation level dependent (BOLD) contrast and inflow effect from relatively large veins were thought to be the contrast mechanism of fMRI, especially in the clinically available 1.5 T MRI system.[6–9] Previous fMRI studies have demonstrated that functional signal change within the visual cortex in infants shows negative response to photic stimulation.[10] However, visual function of neonates is poorly understood. To determine developmental changes of activity-related metabolism in human visual cortex, we performed fMRI from the neonatal period.

Materials and Methods

We studied 15 infants (8 males and 7 females), corrected for gestational age at birth (Table 1), aged less than 1–54 weeks, whose perinatal risk factors warranted screening for possible brain damage. Seven infants had been born pre-term. Informed consent was obtained from the parents.

All infants were sedated with pentobarbital 3–5 mg/kg injected intravenously. The peripheral pulse rate and respiratory rate were monitored, and the infants were closely observed in the MRI unit. Other than the constant gradient noise of echo planar imaging and the photic stimulation, other sensory stimuli were minimized. Patients' eyes were closed during the study. MRI was performed with a 1.5 T MRI system (Signa Horizon, GE) using a standard birdcage head coil. With the use of sagittal T2-weighted spin echo images (repetition time (TR) of 3 s; echo time (TE) of 88 ms; matrix size 256 × 256, a field of view (FOV) of 240 mm) as an anatomical guide, five axial slices approximately parallel to the calcarine fissure were selected for the activation studies. For $T2^*$-weighted fMRI, 102 consecutive gradient-echo echo planar image sequences were acquired with TR/TE of 3 s/50 ms, a flip angle of 90°, a FOV of 220 mm, a 128 × 128 image matrix, and a slice thickness of 5 mm (voxel size: 1.7 × 1.7 × 5 mm). An initial baseline phase of rest for 30 s was followed by a photic stimulation phase alternating with a rest phase, with a total of 10 phases per trial. Visual stimulation was performed with 8 Hz flickering light projected onto the sedated infant's eyelids. Eighty data sets were analyzed, with 22 sequences as prescan data points. The statistical significance of each voxel's response was calculated

Table 1. Summary of results

Patient	Gestational age (weeks)*	Age at fMRI (weeks)		SPM outcome in visual cortex	
		Corrected	Chronological	Max Z value**	Activated voxels
1	38	<1	2	4.52	99
2	40	2	2	4.59	206
3	40	2	2	4.61	224
4	42	3	1	4.19	263
5	30	3	13	4.56	423
6	29	5	16	5.99	425
7	40	8	8	−5.22	622
8	32	16	24	−3.68	69
9	38	16	18	−4.88	428
10	34	17	23	−4.39	225
11	35	18	23	−4.53	371
12	29	22	33	−4.59	514
13	36	28	32	−4.69	505
14	40	53	53	−4.26	238
15	40	54	54	−4.34	110

*Gestational age was calculated from the mother's last memoposal period. **Minus value means a negative response.

with statistical parametric mapping (SPM) (using software from the Welcome Department of Cognitive Neurology, London, UK) implemented in Matlab (Mathworks, Inc., Sherborn MA, USA).[11,12] The images from each subject were realigned using the first image as a reference. After realignment, spatial smoothing to a full width at half maximum of 5, 5, 10 mm for the X, Y, Z axis respectively, was performed. Finally, voxel-wise statistical analysis was performed using the general linear model (with temporal smoothing and autocorrelation over time) and statistical inference based on the spatial extent and maxima of thresholded activation foci using the theory of Gaussian fields. Significance was defined as $p < 0.05$. The threshold of SPM(Z) was set at 2.8 with correction for multiple comparisons to keep the false-positive rate at the defined level ($p < 0.05$).

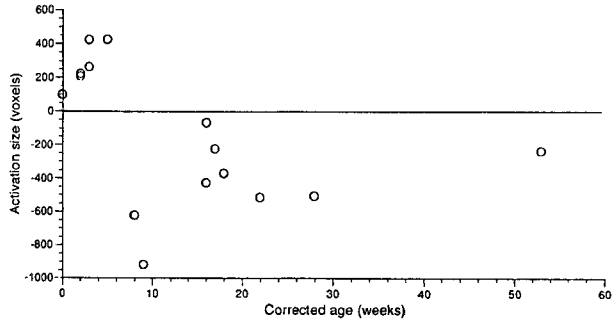

FIG. 1. Significantly activated voxels as a function of age for all 15 infants.

Results

In all subjects, a stimulus-related signal change was observed in the anterolateral region of the calcarine fissure. Although the anatomical distribution of activated voxels was similar in all subjects, fMRI revealed distinctly different patterns of stimulus-related signal changes in neonates less than 5 weeks of age and older infants. Fig. 1 shows the size of activated voxels as a function of age for all subjects. Six neonates less than 5 weeks of corrected age showed a stimulus-related signal increase in the occipital cortex, as in a previous study of human adults (adult pattern, Fig. 2a). Eight infants older than 8 weeks of corrected age showed a stimulus-related signal decrease, which is opposite to that of the normal adult pattern (Fig. 2b). Two premature subjects older than 8 weeks of postnatal (chronological) age, but less than 5 weeks of corrected age, showed a positive response to photic stimulation (patients 5 and 6 on Table 1).

Discussion

This is the first report showing that activity-related metabolism in human cerebral cortex alters rapidly early in life. Developmental changes of cerebral blood flow and glucose metabolism have been reported.[4,5,13] Average global cerebral blood flow and cerebral oxygen utilization in normal children were approximately 1.8 times and 1.3 times as large, respectively, as those in normal young adults.[13] In the neonatal period (less than 4 weeks of age), the most prominent glucose consumption rate (cerebral metabolic rate of glucose; CMRGlu) was found in the primary sensorimotor area, and the remaining cerebral cortical regions showed relatively lower metabolic activity.[4,5] By approximately the second month of age, CMRGlu had increased in calcarine and temporal cortices.[4,5]

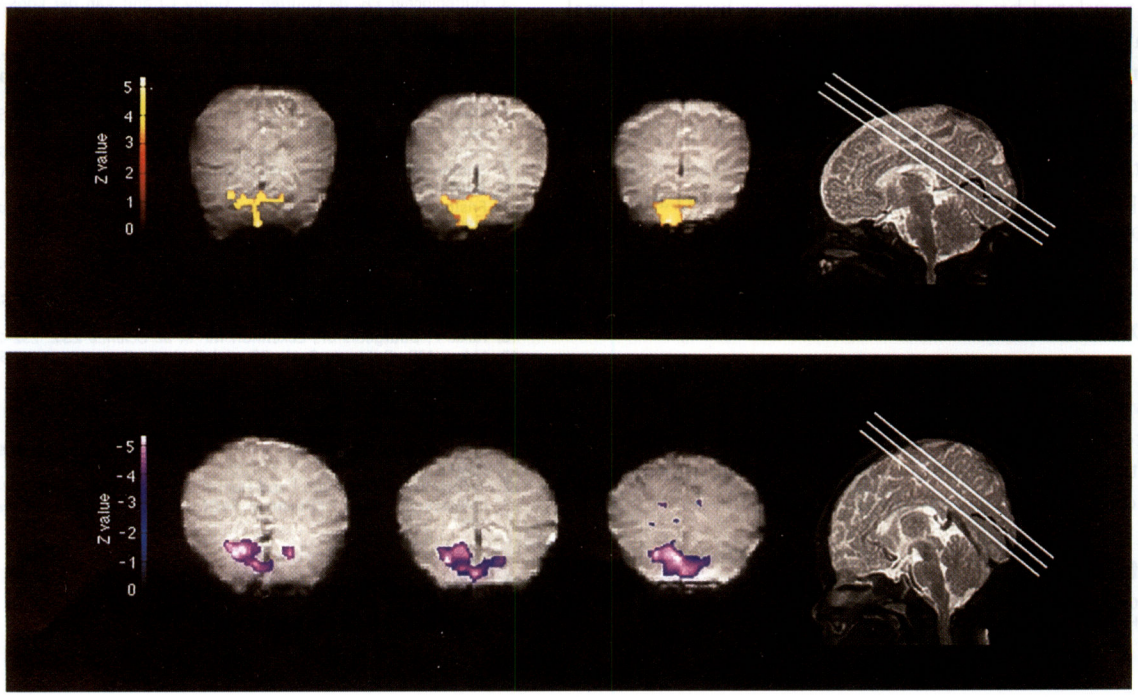

FIG. 2**a**. Functional MRI (left) and reference sagittal T2-weighted image (right) of patient 3, a neonate of 3 weeks corrected aged. The oblique white lines in sagittal image indicate the plane of echo planar images, located along the bank of the calcarine fissure (curved black line). A statistical parametric map of this subject was superimposed onto the subject's original 3 echo planar images parallel to the calcarine fissure. Red and yellow indicate areas with significant positive correlation with visual stimulation in the occipital cortex. **b**. Functional MRI and reference sagittal image of patient 7, an 8-week-old infant. Blue and purple indicate areas with significant negative correlation with visual stimulation in the primary visual cortex.

Considerable rises in CMRGlu were observed in the calcarine cortex by approximately 3 months postnatally.[4,5] These findings support the concept that a rise in the metabolic rate of a particular structure marks the time of its contribution to behavior. Actually, by the third month of age, normal infants can follow the motion of a mother's hand.[14]

We observed different fMRI responses to photic stimulation in the occipital cortex: a signal increase in neonates younger than 5 weeks of age and a signal decrease in older infants. The mechanism of the positive signal change has generally been interpreted as a reflection of an increase in blood oxygenation due to an excessive increase in cerebral blood flow with an oxygen supply in excess of metabolic demands.[6,7] The blood oxygen level dependent (BOLD) technique[6,7] would show a negative effect if an increase in oxygen consumption of the neurons with increased activity is not compensated by the flow of blood. During development, the brain produces a vast excess of neurons, synapses, and dendritic spines.[3,15–18] The overproduction of neurons and synapses is advantageous in the adaptation and plasticity of the brain. Huttenlocher *et al.*[3] determined age-related changes in synaptic density in the human primary visual cortex. They defined a period of rapid synapse production that starts postnatally at the age of 2 months and a subsequent period of synapse elimination that extends past the age of 3 years. LeVay *et al.*[19] and Wiesel[20] have demonstrated that monocular deprivation performed during the early stages of postnatal development dramatically affects the functional organization of the visual cortex. They termed this the 'critical period' during which synaptic connections in the primary visual cortex are modified by visual experience. The experience in human infants with cataract removal indicates that visual acuity may be impaired after 2 months of age, even if cataract removal is successful.[21,22] A negative response to visual stimuli in the occipital cortex was observed in the period between postnatal ages 2 and 13 months, which corresponds well with the period of rapid formation of synapses and rapid increase of CMRGlu in human visual cortex.[3–5] It is therefore very likely that in fMRI the reverse signal response in neonates and infants represents the excessive production of synapses, which results in a rapid increase of oxygen and glucose demand. As shown in premature infants, patients 5 and 6, the inversion of the signal response depends on the age corrected for gestational age at birth, not on chronological age. This finding suggests that a rapid increase in metabolic and synaptic activity in the occipital cortex may not depend on the length of light exposure. This is consistent with a previous study in rhesus monkeys.[15] The ascending phase of synapse overproduction may

be regulated by a common genetic or humoral signal that is relatively independent of the age of onset and duration of visual stimulation.[15] The effect of sedation by pentobarbital, as used in this study, on the MRI signal would be minimal because adults sedated with pentobarbital showed an increased signal in response to visual stimulation,[23] and because our protocol for sedation with pentobarbital was identical in all subjects.

Conclusion

By establishing changes in fMRI during normal development, it will be possible to use fMRI for the detection of visual and other functional impairments in the early infantile period and for the noninvasive study of plasticity of the human CNS.

References

1. Chi JG, Dooling EC and Gilles FH. *Ann Neurol* **1**, 86–93 (1977).
2. Herschkowitz N. *Biol Neonate* **54**, 1–19 (1988).
3. Huttenlocher PR, de Courten C, Garey LJ and Van der Loos H. *Neurosci Lett* **33**, 247–252 (1982).
4. Chugani HT and Phelps ME. *Science* **231**, 840–843 (1986).
5. Chugani HT, Phelps ME and Mazziotta JC. *Ann Neurol* **22**, 487–497 (1987).
6. Ogawa S, Tank DW, Menon R *et al. Proc Natl Acad Sci USA* **89**, 5951–5955 (1992).
7. Kwong KK, Belliveau JW, Chesler DA *et al. Proc Natl Acad Sci USA* **89**, 5675–5679 (1992).
8. Belliveau JW, Kennedy DN, McKinstry RC *et al. Science* **254**, 716–719 (1991).
9. Sereno MI, Dale AM, Reppas JB *et al. Science* **268**, 889–893 (1995).
10. Born P, Rostrup E, Leth H *et al. Lancet* **347**, 543 (1996).
11. Friston KJ, Worsley KJ, Frackowiak RSJ *et al. Hum Brain Mapp* **1**, 210–220 (1994).
12. Friston KJ *et al. NeuroImage* **2**, 45–53 (1995).
13. Kennedy C and Sokoloff L. *J Clin Invest* **36**, 1130–1137 (1957).
14. Bronson G. *Child Dev* **45**, 873–890 (1974).
15. Bourgeois JP, Jastreboff PJ and Rakic P. *Proc Natl Acad Sci USA* **86**, 4297–4301 (1989).
16. Rakic P, Bourgeois JP, Eckenhoff MF *et al. Science* **232**, 232–235 (1986).
17. Lidow MS, Goldman Rakic PS and Rakic P. *Proc Natl Acad Sci USA* **88**, 10218–1021 (1991).
18. Lidow MS and Rakic P. *J Comp Neurol* **360**, 393–402 (1995).
19. LeVay S, Wiesel TN and Hubel DH. *J Comp Neurol* **191**, 1–51 (1980).
20. Wiesel TN. *Nature* **299**, 583–591 (1982).
21. Beller R, Hoyt CS, Marg E and Odom JV. *Am J Ophthalmol* **91**, 559–565 (1981).
22. Jacobson SG, Mohindra I and Held R. *Br J Ophthalmol* **65**, 727–735 (1981).
23. Loenneker T, Joeri P, Huisman TAGM *et al. Proceedings of the ISMRM* **3**, 1897 (1996).

Received 2 September 1997; accepted 16 September 1997